USING A NOVEL 3D DOUBLE-LAYERED TUMOR SPHEROID SYSTEM TO ASSESSS THE EFFECTS OF PACLITAXEL ON CARTINOMA CELLS

by
Eric Tu Ong

A thesis submitted to Johns Hopkins University in conformity with the requirements for the degree of Master of Science in Engineering

Baltimore, Maryland

June 2017

Abstract

E-Cadherin has been commonly accepted as a tumor suppressor. The E-Cadherin mediated cell-cell junctions prevent individual carcinoma cells to break apart from primary tumor to disseminate into surrounding tissue. Recently, this conventional wisdom has been challenged by clinical studies on breast cancer patients showing that expression of E-Cadherin is associated with poor prognosis. A recent *in vivo* study has demonstrated that E-Cadherin expression functionally supports rapid tumor growth that correlates to a poor clinical outcome. However, due to the difficulty to study tumorigenesis *in vivo* or recapitulate tumorigenicity *in vitro*, the mechanism by which E-Cadherin precedes tumor growth is largely unknown.

In this study, we develop a novel 3D *in vitro* system in which we successfully assembled matrigel and collagen gel to mimic the structure and juxtaposed organization of the basement membrane and stromal extracellular matrix. Our system supports breast cancer cells to grow, to organize their multicellular structure, to invade through the matrigel layer into the surrounding collagen I matrix and to organize neighboring stromal tissue. Our 3D system allows us to continuously monitor cell proliferation, invasion, collective migration, and tumor growth simultaneously. We utilize the system to observe E-Cadherin expression and paclitaxel response on carcinoma cells. Our current results indicate the presence of E-Cadherin changes multicellular organization and the invasion of cancer cells, leading to faster tumor growth and increasing the half-maximal inhibitory concentration of paclitaxel.

Advisor: Dr. Denis Wirtz

Committee: Dr. Denis Wirtz and Dr. Daniele Gilkes

Acknowledgements

First and foremost, I want to give my sincere thanks to my mentor and advisor, Dr. Denis Wirtz. He always pushed me to think critically and analyze my data from many different perspectives. The questions he ask and experiments he propose always make me think outside the box, to not only be a good scientist but also a great analyst. He constantly supported me, and shaped the way I approach scientific questions. His dedication to science and its applications inspire me every day, and has been a role model for me since I began independent research. I would not be where I am today without him. It has been a privilege to work in his lab.

I would also like to thank members of the Wirtz Lab for their support and encouragement during the past year as I have pursued my Master of Science and Engineering in Chemical and Biomolecular Engineering. Everyone has been incredibly supportive and constantly pushes me to become a better scientist. I want to especially thank Dr. Meng Horng Lee, the post-doctoral fellow that I have the privilege of working with for the past two years. His scientific expertise and interpersonal skills have made my time in lab especially enjoyable and rewarding.

Finally, I would like to thank my family who has been there for me every step of the way. I would not be the person I am today without their unconditional love and support in everything I do. They have always given me the freedom to pursue my passion and interests, and I am beyond grateful for the trust they have placed in me.

Table of Contents

List of Acronyms

3DLTS	3D Double-Layered Tumor Spheroid System
DIC	Differential Interference Contrast Microscopy
ECM	Extracellular Matrix
EMT	Epithelial-Mesenchymal Transition
ER	Estrogen Receptor
HER2	Human Epidermal Growth Factor Receptor 2
IBC	Inflammatory Breast Carcinoma
IC_{50}	Half Maximal Inhibitory Concentration
MDA	MDA-MB-231 Cell Line
MDA+E-Cad	MDA-MB-231 Cell Line with E-Cadherin Expression
MDA-wt	MDA-MB-231 Cell Line without E-Cadherin Expression
MET	Mesenchymal-Epithelial Transition
PR	Progesterone Receptor
PTX	Paclitaxel
RFS	Relapse-Free Survival
RFU	Relative Fluorescence Units
SE	Standard Error
SEM	Standard Error of the Mean

List of Figures

Introduction

1.1 Breast Cancer Overview

Breast cancer is the most common cancer that occurs in women. In 2017, more than 294,000 patients are expected to be diagnosed in the US, equating to about 30% of all cancers[1]. This means that 1 in 8 women in the US will develop invasive breast cancer during her lifetime. Additionally, breast cancer is still the 2nd leading cause of cancer-related deaths for women in the United States (Fig. 1). Although the number of deaths have decreased by 34% since 1990, in 2017, more than 40,000 women are still predicted to die from breast cancer[1]. A woman's risk of breast cancer nearly doubles if she has a first-degree relative who has also been diagnosed. About 5-10% of breast cancers can be linked to inherited gene mutations, most commonly in the BRCA1 and BRCA2 genes[2]. Upon diagnosis, the patient's treatment options are determined by the presence or absence of three key receptors: ER, PR and HER2, as well as clinical staging based on size, lymph node involvement and tumor histology. Despite all of these evaluations, there are still no techniques of definitively identifying patients who will relapse or whose tumor will metastasize[3]. Consequently, there is still very little we can do to improve the prognoses for these types of patients.

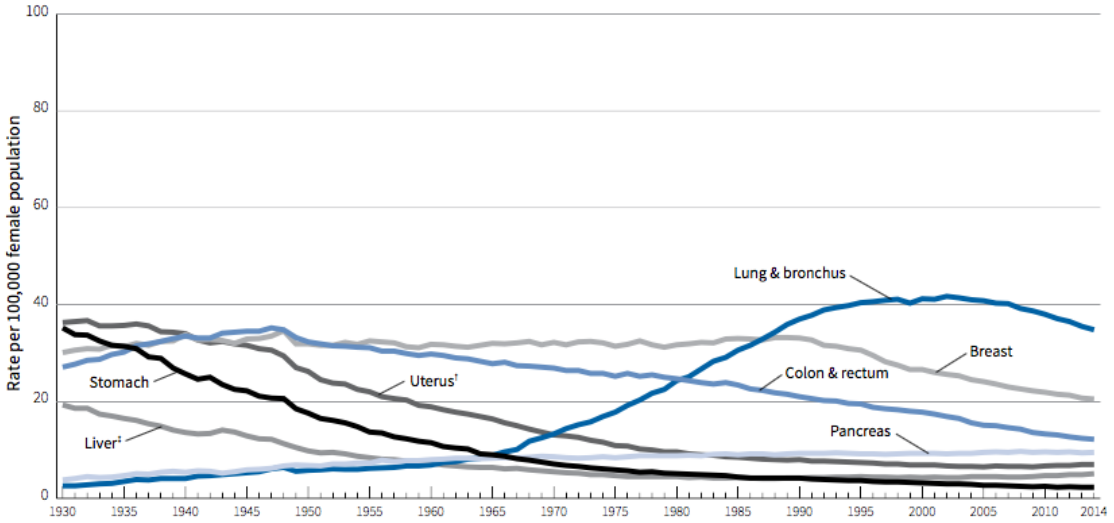

Figure 1: Trends in age-adjusted cancer death rates by site, females, US, 1930-2014[1]. According to the American Cancer Society, in 2016, breast cancer remains the second leading cause of death among women in the United States.

1.1.1 Tumorigenesis

How cancer cells form tumors has been a riddle in science for decades. Specifically, how cancerous cells recruit other cancerous cells and healthy cells into its immediate niche to form tumors is a complex process to understand. The field cancerization effect suggests that tumor growth could be mediated, at least in part, by the coalescence of multiple tumorigenic foci within a tissue, a process that would contribute to tumor heterogeneity[4].

Studies have been done to offer key insights on how and why tumors form by recording in real time, and in 3D, the movement of cancerous human breast tissue cells[5]. This computer-assisted *in vitro* model for reconstructing 3D cell behavior was able to continuously track cancer cells' motion and accretion into tumors. Researchers discovered that cells from tumorigenic cell lines and fresh tumors when seeded in a 3D matrigel matrix grow into clonal-island like primary aggregates[5]. Then these larger

aggregates undergo morphogenesis to generate a highly structured, large spheroid. The coalescence process is facilitated by specialized cells that exit neighboring aggregates, forming cellular cables between the primary aggregate. The cables then contract, moving smaller aggregates into larger ones. This active process continues, generating a final large aggregate that undergoes differentiation[5]. Researchers consistently found evidence of this behavior for cells from tumor tissues and cell lines from a variety of cancers. While on the other hand, non-tumorigenic, or weakly tumorigenic lines and cells from healthy control tissues would form clonal islands in the 3D matrigel through cell multiplication, but would fail to generate the specialized cells and undergo coalescence[5].

Researchers also investigated the possibility that tumor heterogeneity, mixtures of majority non-tumorigenic cells and minority tumorigenic cells, may not only be due to the differentiation of cells within a tumor, but also to the active recruitment of non-tumorigenic cells by tumorigenic cells into the tumor[5]. They tested the tumorigenic breast cancer cell line, MoVi-10', which was engineered through overexpression of intermediate filament vimentin, and a weakly tumorigenic parental breast cancer cell line MCF-7[5]. They found, surprisingly, that as little as 5 % of tumorigenic MoVi-10' cells will actively cause primary aggregates of majority MCF-7 cells to undergo coalescence (Fig. 2). Again, it was demonstrated that coalescence is mediated by the formation of cables composed entirely of minority MoVi-10' cells, and these cellular cables contract, pulling smaller aggregates of non-tumorigenic cells into larger aggregates.

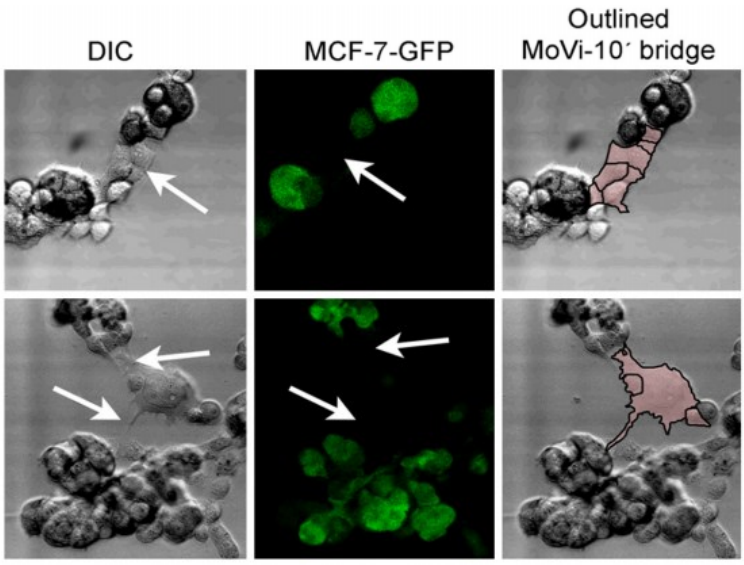

Figure 2: Minimal MoVi-10' cells will cause coalescence of majority MCF-7 cell primary aggregates through cellular bridges[5]. 90% MCF-7 cells expressing green fluorescent protein were mixed with 10% unlabeled MoVi-10´ cells and seeded in 3D matrigel. DIC image (left) shows all cells forming primary aggregates attached by cellular bridges, while MCF-7-GFP (middle) shows view only MCF-7 cells. Note the bridges between primary aggregates (white arrows) were consisted of only unlabeled MoVi-10´ cells. This shows cellular bridges are formed exclusively by non-fluorescent MoVi-10´ cells, and the outlined pink bridges (right) show the unlabeled MoVi-10' cells forming the connection[5].

In other words, cancerous cells actively recruit healthy cells into tumors by extending a cable of sorts to grab their neighbors – both cancerous and healthy – and reel them in. Furthermore regardless of the ratio of MoVi-10' to MCF-7 cells in the cluster, only MoVi-10' cells reached out and drew in other cells, including cancerous and healthy cells, to the growing mass[5]. These results suggest an alternative mechanism for the presence of a high percentage of non-tumorigenic cells within a given tumor, and thus provide an additional perspective on how tumor heterogeneity may arise *in vivo*. This explanation of tumor formation also shed insight on how tumors are created concurrently, in multiple locations, by individual clusters of cells that employ the cancer-cell cables to draw in more cells and enlarge themselves[5]. It further elucidates information on tumor formation, and how a well-built 3D *in vitro* tumor spheroid system can be used to study tumor

morphology, and transformation of carcinoma cells in matrigel into clonal-island like primary aggregates and structured spheroids.

1.2 E-Cadherin

Cellular adhesion and motility is one of the critical mechanisms that control tumor initiation, progression, and growth[6]. Researchers have done many studies on understanding how adhesive dysfunction contributes to cancer biology, building upon the classic demonstration that tumor cells adhere to one another less avidly than non-tumor cells do[7]. These studies led to the discovery of cadherin cell-cell adhesion receptors, which are key regulators of tissue architecture during development and in tissue homeostasis, providing a group of molecular candidates to link cell-cell adhesion, morphogenesis, and cancer[6,7].

As a family of cell surface glycoproteins, cadherins play a critical role in cell-cell adhesion and act as a key structural component of adherens junctions, modulating Ca^{2+} dependent and homophilic cell-cell adhesion via extracellular domains[8]. In addition, they link the cytoskeleton to the extracellular environment, and participate in cell signaling through interactions of their conserved cytoplasmic domains with catenin, particularly p-120, α, and β-catenin[8]. This is accomplished by β-catenin binding directly to the distal region of the cytoplasmic tail; while α-catenin is indirectly coupled to the cadherin complex by association with β-catenin; and p-120 catenin that binds to the membrane-proximal region of the cadherin cytoplasmic tail. Through this signaling pathway, cadherins interact with a range of proteins that link the receptor to fundamental intracellular processes, including cell trafficking, nucleation, filament dynamics, and

crosslinking. E-Cadherin, a type I classical cadherin, is a key component in the formation of many cell-cell adherens-type junctions in epithelial tissues. The calcium-dependent interactions among E-Cadherin molecules are critical for the formation and maintenance of these junctions in areas of epithelial cell-cell contact (Fig. 3)[9].

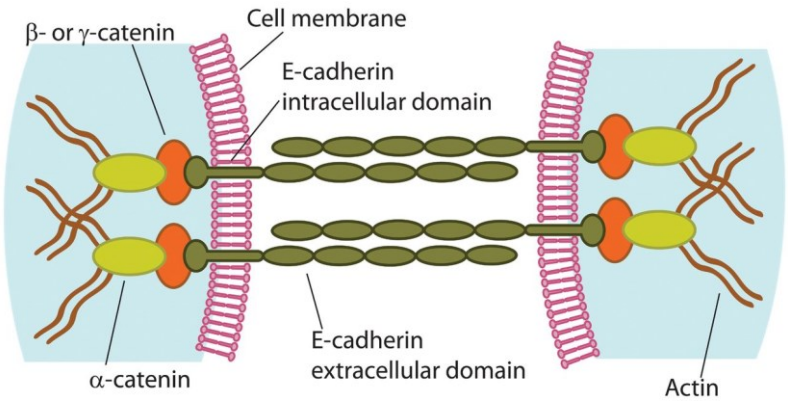

Figure 3: E-Cadherin and the adherens junction[9]. The extracellular domains of E-Cadherin homodimers enter homotypic Ca^{2+}-dependent-binding interactions with those of dimers on adjacent cells. The intracellular domain of E-Cadherin interacts with the actin cytoskeleton via α-catenin and either β- or γ -catenin. Cadherin–catenin complexes constitute the adherens junction[9].

1.2.1 E-Cadherin expression and tumor growth

E-Cadherin has been commonly categorized as a tumor suppressor, given its essential role in the formation of intercellular junctions, and its downregulation in the process of epithelial-mesenchymal transition (EMT) in epithelial tumor progression. Loss of E-Cadherin-mediated-adhesion characterizes the transition from benign lesions to invasive and metastatic cancer[8].

At the experimental level, E-Cadherin's function as a tumor suppressor is demonstrated through suppressing its expression that leads to mesenchymal morphology, increased cell migration and invasion, as well as metastasis[8,9]. This leads to the initial invasive behavior of certain epithelial-derived cancers and is thought to be the cause of

basement membrane transgression and spread[10]. The EMT is a developmentally important process which includes a spectrum of changes that lead to downregulation of epithelial cell traits such as apical-basal polarization and organized cell-cell adhesion, as well as acquisition of a mesenchymal cellular phenotype that is less adherent and more migratory[10,11]. Together, these changes lead to tissue reorganization and morphogenesis during cancer development. It is increasingly apparent that aspects of the EMT underlie the progression of carcinomas toward increasingly malignant states. One component of the EMT process is the cadherin "switch" in which the expression of epithelial cadherins (e.g. E-Cadherin) is down regulated and conversely mesenchymal cadherins (N-cadherin) are expressed (Fig. 4)[12].

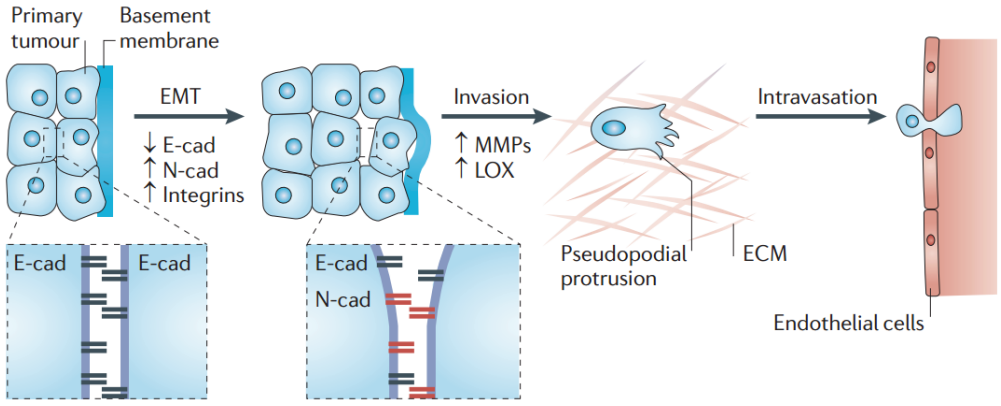

Figure 4: Downregulation of E-Cadherin and the EMT[12]. The EMT is associated with a loss of adhesion through downregulation of E-Cadherin, upregulation of N-Cadherin, and a change in morphology. This causes detachment from the primary tumor, and subsequent invasion of the surrounding tissue caused by the physiochemical properties of the extracellular matrix. These processes lead toward invasion, intravasation, and metastasis[12].

These switches are experimentally linked to increase cell motility and the ability to invade and/or metastasize. It is in this context that E-Cadherin's tumor suppressor role in cancer is most often viewed. In the most simplified model, E-Cadherin's presence

prevents cell motility, invasion, and metastasis, thus may prevent the formation of cells to tumor state[12].

1.2.2 E-Cadherin expression in tumor progression and in clinical observation

Although E-Cadherin's role as a tumor suppressor is established with firm supporting experimental evidence, in recent years, alternative roles for E-Cadherin in tumor progression, in particular with respect to tumor context and specific mechanisms, have become apparent[7]. In some cases, like the formation of tumor emboli that is seen in inflammatory breast cancer (IBC), cadherin-based cell-cell contacts may promote tumor cell survival, growth, and invasion. The process of collective cell migration, which is also important in epithelial cancers, requires intact E-Cadherin and proper intercellular junctions. Furthermore, studies have begun to understand the maintenance or re-acquisition of an epithelial phenotype as well as the reversion to a mesenchymal-to-epithelial (MET) phenotype, defined by the expression of E-Cadherin, as a requirement for tumor colonization at sites distant from the primary tumor[7,8]. For instance, while an EMT does occurs in breast carcinoma, evidence has been seen that E-Cadherin also plays an important role in maintaining intravasated microemboli in IBC models, thus facilitating tumor intravasation, the invasion of cancer cells through the basal membrane into a lymphatic vessel. This carcinogenic event initiates the escape of cancerous cells from their primary sites, into distant locations. Despite IBC's aggressiveness, E-Cadherin expression is maintained in the primary tumor and tumor emboli[10]. Thus, this model represents the prototype breast cancer with prominent MET behavior. These observations

suggest that E-Cadherin expression is not solely confined to tumor suppression, but instead may have a role in promoting role in tumor progression and growth as well[11].

Recent clinical observation has also shown E-Cadherin expression correlates to a poor clinical outcome in patients with breast cancer[6]. Two groups were analyzed: patients with E-Cadherin expression above the mean were considered high expressors, and those below the mean were designated as low expressors. High expression of E-Cadherin was associated with poor relapse-free survival (RFS) (Logrank P = 0.032 and Logrank P = 0.025) (Fig. 5)[6]. Patients with high expression of E-Cadherin were associated with poor RFS, the length of time after primary treatment for a cancer ends that the patient survives without any signs or symptoms of that cancer, in primary basal breast tumors. This positive association between poor prognosis and E-Cadherin expression is seen in ovarian cancer and IBC, as well as numerous models of metastatic cancer[6].

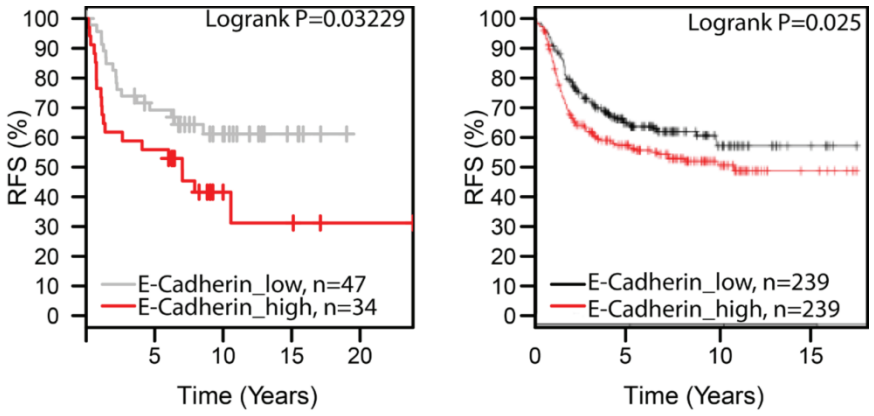

Figure 5: E-Cadherin expression correlates to a poor clinical outcome in patients with breast cancer[6]. Kaplan-Meier curve depicting the correlation between E-Cadherin expression and relapse-free survival (RFS) in primary basal breast tumors using two public databases of breast cancer microarrays. Logrank P values are indicated[6].

With the conventional wisdom of E-Cadherin as a tumor suppressor challenged by clinical studies of breast cancer patients showing that the expression of E-cadherin is associated with a poor clinical prognosis, the paradox of E-Cadherin remains complex as the mechanism by which E-cadherin facilitates tumor growth is largely unknown due to the difficulty to recapitulate tumor growth *in vitro*.

1.3 Paclitaxel

Paclitaxel (PTX) is a microtubule-stabilizing drug that is approved by the Food and Drug Administration for treating a variety of cancers, including breast, ovarian, and lung cancer[13]. It is also used off-label to treat gastroesophageal, endometrial, prostate, cervical, and head and neck cancers, in addition to sarcoma, lymphoma, and leukemia. It is one of the most commonly used chemotherapy drugs, and is listed on the World Health Organization's List of Essential Medicines, the most effective and safe medicines needed in a health system[14]. Paclitaxel has long been recognized to induce mitotic arrest, which leads to cell death in a subset of the arrested population. It promotes microtubule polymerization and stabilization in living cells and in its treatment arrests a diverse array of cell types in mitosis, in both animal tumor models and cell culture[13].

Paclitaxel-induced mitotic arrest happens due to the activation of the mitotic checkpoint, also known as the spindle assembly checkpoint. This is the major cell cycle control mechanism acting during mitosis to prevent chromosome missegregation[13]. The checkpoint delays separation of the chromosomes, which enter mitosis as replicated pairs of sister chromatids, until each pair has made stable attachments to both poles of the

mitotic spindle. Paclitaxel treatment arrests cells in mitosis due to the presence of a small number of unattached kinetochores (Fig. 6)[13].

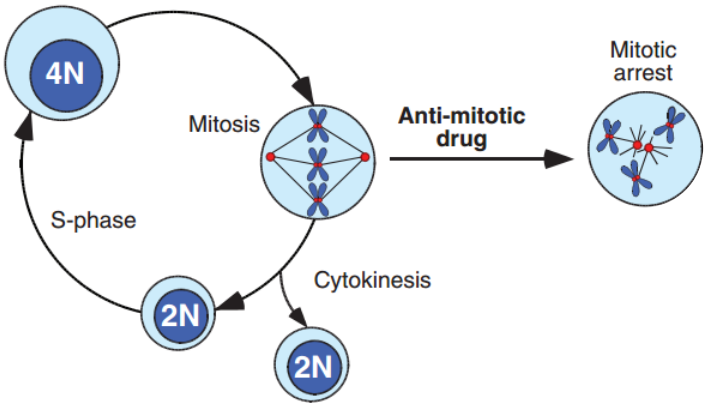

Figure 6: Paclitaxel induces mitotic arrest[13]. Paclitaxel, an anti-mitotic drug, binds to microtubules resulting in their stabilization via suppressing their dynamic changes. Thus, Taxol interferes with the formation of mitotic spindle, which causes the chromosomes not to segregate and consequently mitotic arrest[13].

From both *in vitro* and *in vivo* studies, Paclitaxel-loaded microspheres have shown to induce tumor apoptosis and inhibit the establishment and growth of cancerous cells[14].

1.4 3D Double-Layered Tumor Spheroid System (3DLTS)

1.4.1 The need for a novel *in vitro* tumor model

In vitro tumor models over the years have provided important tools for cancer research, and serve as low-cost screening platforms for drug therapies. However, cancer recurrence remains largely unchecked due to metastasis, which is the major cause of cancer-related deaths. The current *in vitro* systems available today, whether in 2D or 3D culture, are sufficient in providing critical tumor cell proliferation, invasion, and migration information. Yet, these models often stop short and are limited in

understanding true tumor growth and morphology. There is a disconnect in the currently available systems to develop and understand the mechanism behind tumor growth. The need for an improved understanding of the progression and treatment of cancerous tumors has pushed for increased accuracy and physiological relevance of *in vitro* tumor models[15].

As a result, there is a need for a novel *in vitro* tumor model to recapitulate critical steps in the metastatic cascade, such as intravasation, extravasation, and extracellular matrix and stroma remodeling. The development of new *in vitro* tumor models will enable researchers to incorporate multiple cell types, of different cancers, and of different tumor density to simulate the tumor vasculature. These advancements will lead to adapting *in vitro* tumor models for patient-specific therapies of precision medicine, to allow scientists and physicians to use *in vitro* models for drug screening purposes[15].

1.4.2 3D Double-Layered Tumor Spheroid System (3DLTS)

In this project, we develop a novel 3D *in vitro* system, 3D double-layered tumor spheroid system (3DLTS), in which we successfully assembled matrigel and collagen gel to mimic the structure and juxtaposed organization of the basement membrane and stromal extracellular matrix (ECM). Our goal is to develop a system to more closely monitor the tumor growth and morphology in the tumor microenvironment (Fig. 7). In the immediate area surrounding carcinoma cells is the basement membrane which we mimic with matrigel. Surrounding the carcinoma cells embedded in matrigel would be the stroma area which is in collagen I rich matrices.

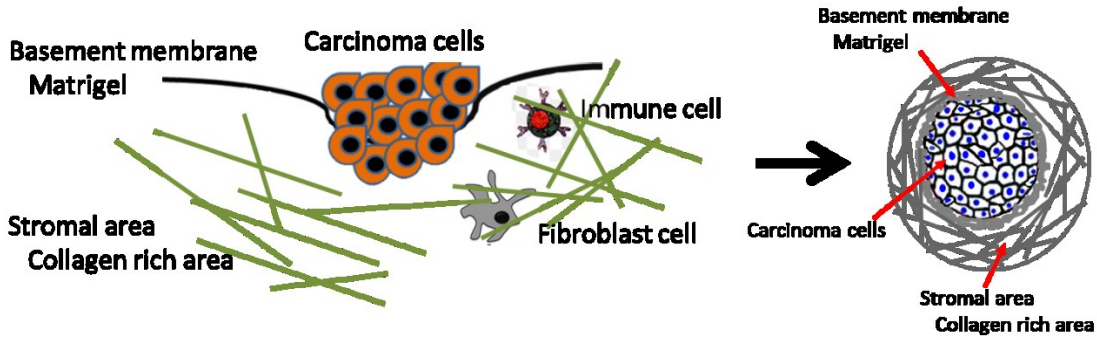

Figure 7: Tumor microenvironment and 3DLTS. Cartoon depicts the usual tumor microenvironment (left) with carcinoma cells embedded in basement membrane and stroma area. We recreate this microenvironment in our 3DLTS (right).

Our system supports breast cancer cells to grow, to organize their multicellular structure, to invade through the matrigel layer into the surrounding collagen I matrix and to organize neighboring stromal tissue. Our 3D system allows us to continuously monitor cell proliferation, invasion, and collective migration simultaneously. Through our imaging system and cell proliferation assays, we are able to capture tumor volume change, stroma volume change, and cell number fold increase over the course of our experiment. We can also monitor the degree of invasion to further understand the mechanism of carcinoma cells invasion into the stroma area (Fig. 8). We utilize 3DLTS to observe E-Cadherin expression and paclitaxel response on breast cancer carcinoma cells (MDA-MB-231, a triple negative breast cancer cell line). We want to observe if the patterns of cell growth in our system are compatible to *in vivo* conditions and clinical observations.

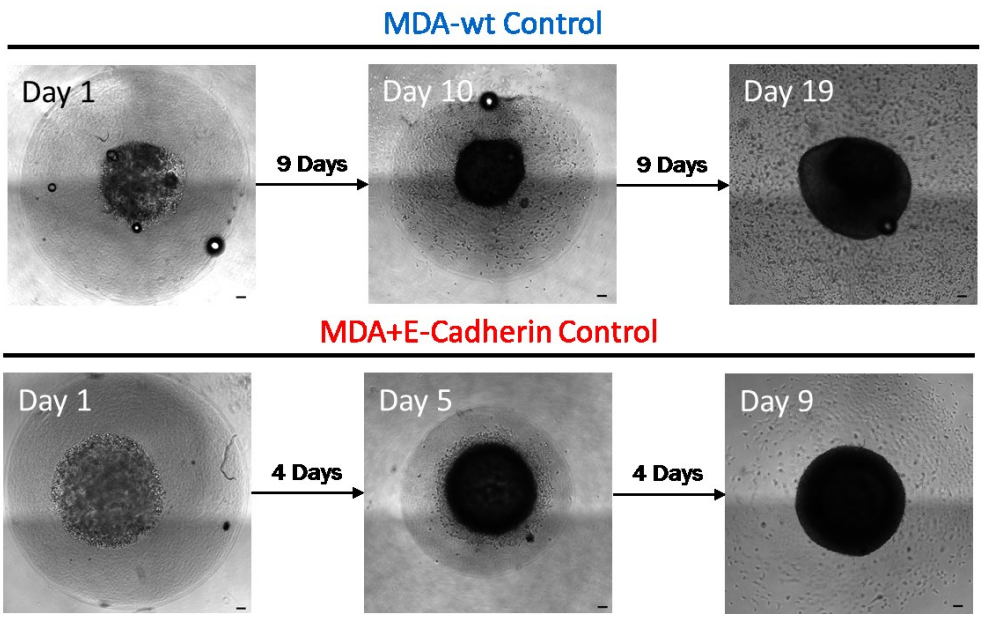

Figure 8: 3DLTS. 3DLTS can monitor tumor volume change, stroma volume change, cell number fold increase, and invasion mechanism by imaging every day. Top: MDA-wt Control shows MDA-MB-231 tumors (triple negative breast cancer cell line) without any drug treatments invade and progress over 19 days. Bottom: MDA+E-Cad Control shows MDA tumors with overexpression of E-Cadherin invade and progress over 9 days. Each unit bar represents 100 µm.

Our system supports breast cancer cells to grow, to organize their multicellular structure, to invade through the matrigel layer into the surrounding collagen I matrix and to organize neighboring stromal tissue. Our 3D system allows us to continuously monitor cell proliferation, invasion, and collective migration simultaneously. We demonstrate that patterns of cell growth in our system are compatible to in vivo conditions. Using our system, we find that the presence of E-cadherin changes multicellular organization and the invasion of cancer cells, leading to faster tumor growth.

1.5 Motivation

The paradox of E-Cadherin as a commonly accepted tumor suppressor gene while its expression lead to worse prognosis in breast cancer patients has shed light on the

complex functions of E-Cadherin. The complex functions of E-Cadherin in retention of an epithelial phenotype and as a mediator of survival of aggressive breast cancer require further understanding through a novel *in vitro* tumor model which can elucidate proliferation, invasion, migration, as well as tumor growth and morphology information.

Thus, we will utilize our 3D double-layered tumor spheroid system (3DLTS) to monitor cell proliferation, invasion, and collective migration under the expression of E-Cadherin. We will also treat the spheroids with paclitaxel to further utilize 3DLTS as a drug screening tool.

Materials and Methods

2.1 Cell Culture

MDA-MB-231 (MDA) cells were obtained from ATCC and cultured in Dulbecco's modified Eagle's medium (DMEM, Sigma Aldrich, St. Louis, MO) supplemented with 10% (v/v) fetal bovine serum (FBS, Corning, Corning, NT) and 1% penicillin-streptomycin (Invitrogen, Carlsbad, CA). Cells were maintained in a humidified environment at 37ºC and 5% CO_2 during culture and live cell imaging.

2.2 Lentiviral expression constructs

The lentiviral vector of enhanced green fluorescent protein (EGFP; pCS-CG) was purchased from Addgene (Cambridge, MA). The lentiviral vector of lifeact-EGFP and E-Cadherin-EGFP were generated from pCS-CG. The sequence of lifeact peptide or full-length E-Cadherin was cloned upstream of EGFP between the Nhe1 and Age 1 sites of pCS-CG to generate EGFP-fused protein. The αE-catenin shRNA vector was generated as described before. Briefly, the sequence 5' -GGACCTGCTTTCG GAGTACAT-3' targeting αE-catenin was cloned downstream of the H1 promoter between the MluI and ClaI sites in pLVTHM lentiviral vector (Addgene, Cambridge, MA).

2.3 Lentivirus production and transduction of MDA+E-Cad

A second-generation lentivirus was produced as described previously. Briefly, MDA-MB-231 cells (ATCC) were transiently cotransfected with three plasmids (lentiviral vector, ΔR 8.91, and pMDG-VSVG) using the standard calcium phosphate precipitation method. After 22–24 hours of transfection, the medium was replaced with

fresh medium. The lentiviral particles were harvested 24 hours later, immediately filtered through 0.45 μm filter (Millipore, Cambridge, MA) to remove cells debris, and then stored at 80° C. For transduction, 1×10^5 MDA-MB-231 cells in a 35-mm culture dish were repeatedly transduced with lentivirus with 8 μg/ml polybrene to reach high transduction (> 80 %). Thus this creates our MDA-MB-231 cells without expression of E-Cadherin (MDA-wt), and MDA-MB-231 cells with expression of E-Cadherin (MDA+E-Cad)

2.4 2D culture of MDA-MB-231 cells

Cells are seeded at a concentration of 10,000 cells/ml in 24 well flat-bottom plate (Corning, Corning, NY). Each well contain 500 μl of cells in Dulbecco's modified Eagle's medium (DMEM, Sigma Aldrich, St. Louis, MO) supplemented with 10% (v/v) fetal bovine serum (FBS, Corning, Corning, NT) and 1% penicillin-streptomycin (Invitrogen, Carlsbad, CA). The plate is incubated at 37ºC and 5% CO_2 over 5 days until cells reach confluence.

2.5 3D double-layered tumor spheres (3DLTS)

To make a 3DLTS, we first mixed 10,000 cancer cells with 0.5 μl matrigel (Corning, Bedford, MA). The mixture was dropped into a spherical mold at 37° C for 30 minutes to allow the gelation of matrigel. Next, we added type I collagen solution (5 μl, Corning, Bedford, MA) to fully cover the first sphere containing cells and matrigel. The mixture was dropped into a spherical mold at 37° C for 1 hour to allow the gelation of

type I collagen. The single 3DLTS was cultured as suspension in a well of 96 well round-bottom dish (Corning, Corning, NY) (Fig. 9).

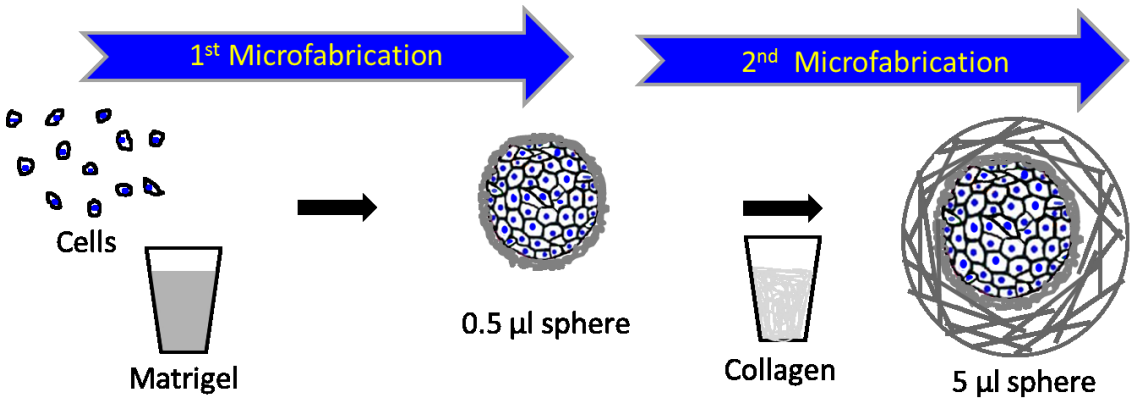

Figure 9: 3DLTS microfabrication process. First, cancer cells are fixed in matrigel, then type I collagen solution was added to cover the first sphere containing cells and matrigel, creating a 5 µl spheroid overall.

To trace cell invasion, time-lapse images were collected every day for 1 week using a Nikon TE2000 microscope equipped with a ×4 objective (Nikon, Melville, NY) and a Cascade 1K CCD camera (Roper Scientific, Tucson, AZ).

2.6 Treatment with Paclitaxel

2.6.1 Paclitaxel treatment on 2D culture

Cells in 24 well flat-bottom plates are treated with 8 nM, 4 nM, 2 nM, 1.5 nM, and 1 nM of paclitaxel (Invitrogen, Carlsbad, CA). On the third day of the five day experiment, suction away 500 µl of drug solution without disturbing the cells adhered on the bottom and replenish with 500 µl of fresh drug solution.

2.6.2 Paclitaxel treatment on 3DLTS

Tumor spheroids in 96 well round-bottom plate are treated with 2 nM, 1 nM, 0.75 nM, 0.5 nM, and 0.25 nM paclitaxel (Invitrogen, Carlsbad, CA) in MDA-wt. In MDA+E-Cad spheroids, they are treated with 4 nM, 2 nM, 1.5 nM, 1 nM, and 0.5 nM paclitaxel. Every four days, we replace 50 µl of the drug solution without disturbing the spheroids and replenish of fresh drug solution.

2.7 PrestoBlue Proliferation Assay

To generate the standard curve of cell number and proliferation rate of MDA-MB-231 tumor spheroids, different numbers of cells per tumor (5,000, 10,000, 20,000, 24,000, and 48,000) were seeded in 96 well round-bottom plates with 100 µl of medium and cultured overnight. Each well was then incubated with 100 µl 1x PrestoBlue reagent (Invitrogen, Carlsbad, CA) for 3 hours with 5% CO_2 at 37°C. 64 µl of cell culture media with PrestoBlue reagent were collected in 96 well flat-bottom plates. The absorbance was measured using the Gemini XPS Microplate Reader (Molecular Devices, Sunnyvale, CA) to generate the following standard curves correlating PrestoBlue relative fluorescence units (RFU) to cell number (Fig. 10).

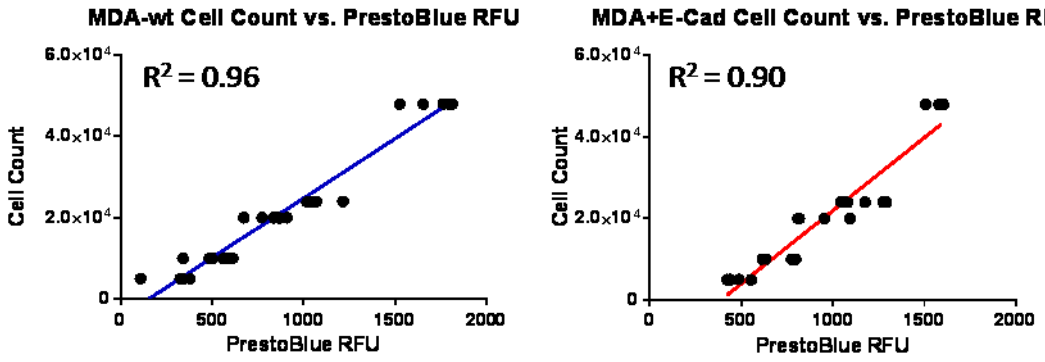

Figure 10: PrestoBlue RFU vs. cell number in 3DLTS. Standard curves correlating PrestoBlue RFU vs. cell number in 3DLTS are generated by seeding different number of cells in the tumor spheroids. For MDA-wt and MDA+E-Cad, the R^2 are 0.96 and 0.90 respectively.

2.8 Measuring 3DLTS Tumor and Stroma Volume

To measure the 3DLTS' tumor volume, we use volume of the sphere formula ($V=\frac{4}{3}\pi r^3$) to get the radius from the projectile imaging to reconstruct into the tumor volume (Fig. 11). Similarly to get the stroma volume, we measure the radius to the outer layer to mark the spheroid volume. The stroma volume would be the spheroid volume subtracts the tumor volume. We would get the two volumes we want to observe from the 3DLTS.

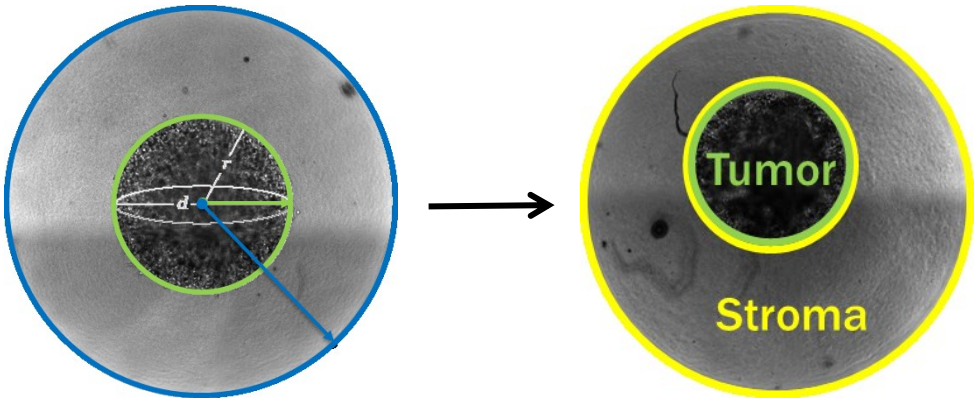

Figure 11: Measuring tumor and stroma volume in 3DLTS. We use volume of the sphere formula to draw the radius from projectile imaging. Left: The green signifies the tumor volume; the blue signifies the spheroid volume. Right: The stroma volume (yellow) would be the spheroid volume subtracts the tumor volume.

2.9 Statistical Analysis

The mean values ± standard error of mean (SEM) were calculated and plotted using GraphPad Prism (6, San Diego, CA) software. When appropriate, statistical analysis were performed to compare means, namely two-tailed unpaired t-tests, one-way

and two-way ANOVA followed by Bonferroni post-tests to determine statistical significance, which is indicated in the graphs as ***$p<0.001$, **$p<0.01$ and *$p<0.05$.

Results and Discussion

3.1 3DLTS recapitulates rapid growth of E-Cadherin tumor

To recapitulate tumorigenesis and to access dynamic change of tumor volume, we utilize the 3DLTS system to assess tumor growth in the invasive human breast carcinoma cell (MDA-MB-231), which does not express E-Cadherin, as a cell model (MDA-wt). As described in the methods, we also employ a gain-of-function approach by supplying E-Cadherin exogenously to MDA-MB-231 cells (MDA+E-Cad). To recap, in our 3DLTS, the central sphere is the mixture of cancer cells and matrigel which replicate the environment of basement membrane. The outer sphere is made by collagen I matrix to mimic stromal tissue and to support the cell invasion and continuous growth of the central tumor sphere.

We measure the tumor volume every day through captured images, and allow the tumors to grow to their maximum volume, categorized by when the tumor and overall spheroid has become a single volume (Fig. 12). The MDA-wt tumor sphere took 18 days to reach its maximum size, while MDA+E-Cad tumors only required 8 days to reach completion.

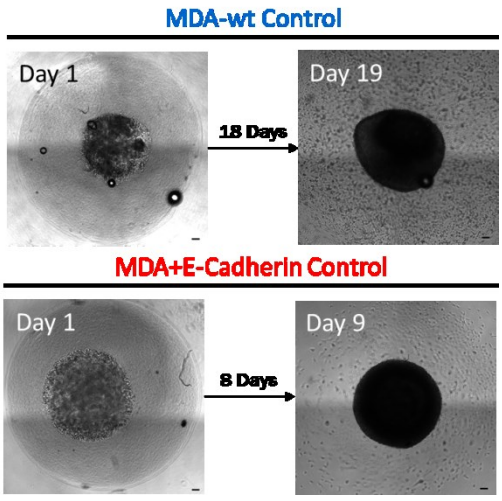

Figure 12: Rapid tumor growth under E-Cadherin expression. MDA-wt require 18 days to grow to their maximum volume, while under E-Cadherin expression, the MDA+E-Cad spheroids only require 8 days to reach their maximum volume.

We plot the normalized tumor volume over the course of the experiment, and found under E-Cadherin expression, the tumor growth is very different (Fig. 13). We found in MDA-wt, tumor compaction occurs until day 6, and then there is a steady tumor growth until it reaches it maximum volume at day 19. On the other hand in MDA+E-Cad, tumor compaction occurs as well, but only until day 3, then there is very rapid tumor growth to allow it reach its maximum volume by day 9.

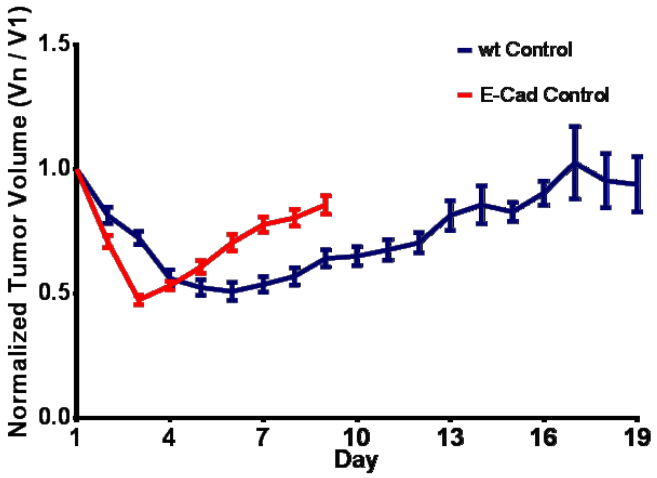

Figure 13: 3DLTS recapitulates rapid growth of E-Cadherin tumor. Under E-Cadherin expression, rapid growth in observed within the 3DLTS.

We also found MDA+E-Cad has nearly a 2.3× greater tumor growth rate compared to MDA-wt (Fig. 14). This is calculated by the fold increase of cell number per day by running the PrestoBlue assay. The much higher increase in cell number per day in the MDA+E-Cad system correlates with the significantly shorter time frame is takes for the MDA+E-Cad tumors to reach completion.

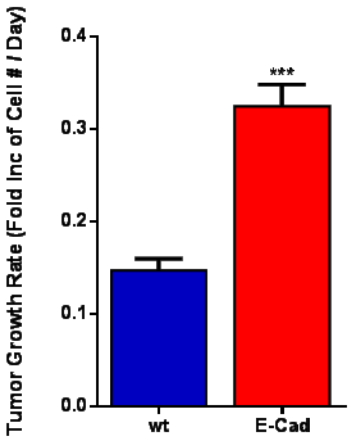

Figure 14: MDA+E-Cad has greater tumor growth rate. Within the 3DLTS, E-Cadherin expression elicits a nearly 2.3× greater tumor growth rate in terms of fold increase of cell number per day compared to MDA-wt.

3.2 E-Cadherin expression accelerates MDA-MB-231 tumor to compact the surrounding stromal tissue

MDA-MB-231 cells have capacity to compact stromal collagen matrix into their tumor sphere. Both MDA-wt and MDA+E-Cad cells compacted outer collagen sphere to form a solid tumor sphere. However, the duration of compaction of MDA-wt tumor was more prolonged than MDA+E-Cad tumor (Fig. 15).

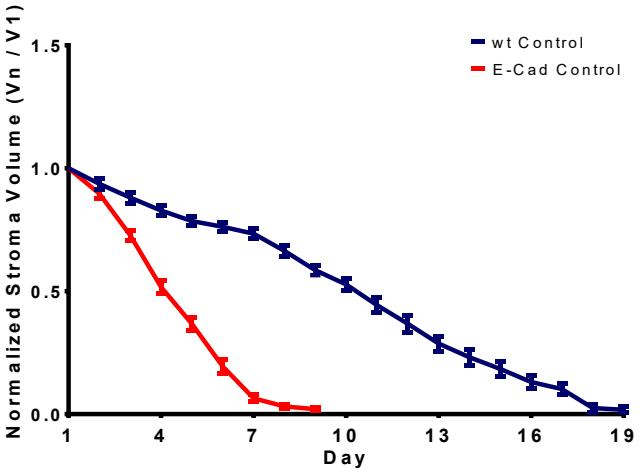

Figure 15: E-Cadherin expression accelerates MDA-MB-231 tumor to contract the surrounding stromal tissue. Under E-Cadherin expression, accelerated stroma contraction is observed within the 3DLTS as compared to MDA-wt.

This rapid stroma compaction observed in MDA+E-Cad correlates with the rapid tumor growth under E-Cadherin expression. We found collagen enrichment is needed for invasion of the tumor cells into the stroma, thus as MDA+E-Cad tumors undergo rapid tumor growth, it quickly pulls in the surrounding stroma to enrich the collagen for active invasion.

3.3 Paclitaxel minimizes tumor growth and stroma volume shrinkage in 3DLTS

We want to observe the effects of paclitaxel on the MDA-wt and MDA+E-Cad tumor growth and stroma volume shrinkage within our 3DLTS. As microtubule-stabilizing drugs that induce mitotic arrest, paclitaxel inhibits tumor growth by disallowing cancerous cells to complete their mitosis cycle in cell replication. This observation is seen in 3DLTS, as paclitaxel is effective in minimizing tumor growth across MDA-wt and MDA+E-Cad tumors at the concentrations we tested (Fig. 16). From the heat map, we can see at increasing drug concentration, the tumor growth is minimized as at day 19 in MDA-wt 2 nM treated tumors, the normalized tumor volume only increased to 0.62, whereas in control it is at 1.10. Similarly, in MDA+E-Cad, at day 9 of the MDA+E-Cad 4 nM treated tumors, the normalized volume increased to 0.52, whereas in control it is at 0.86.

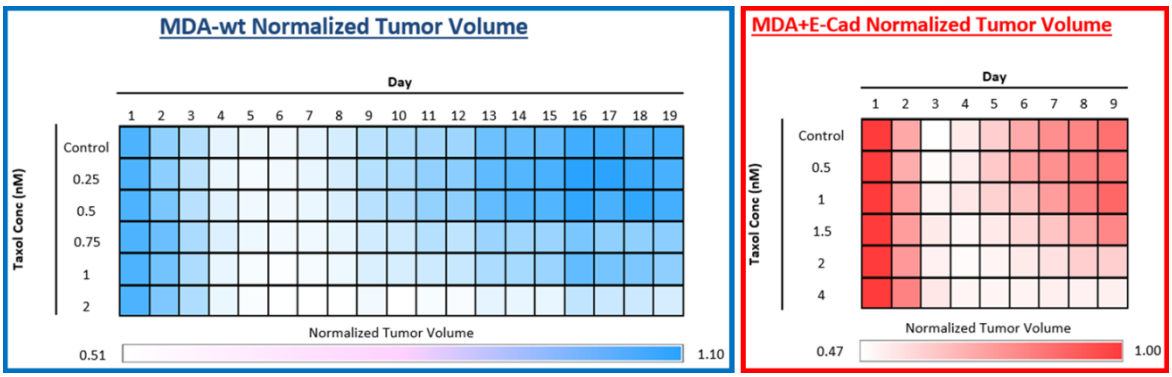

Figure 16: PTX minimizes tumor growth in 3DLTS.

We also want to observe the effects of paclitaxel on stroma volume shrinkage. We see at increasing concentrations of paclitaxel, the stroma volume shrinkage is minimized (Fig. 17). Thus, at the concentrations of paclitaxel we picked for MDA-wt and MDA+E-Cad, they are effective in minimizing tumor growth and stroma volume shrinkage in 3DLTS.

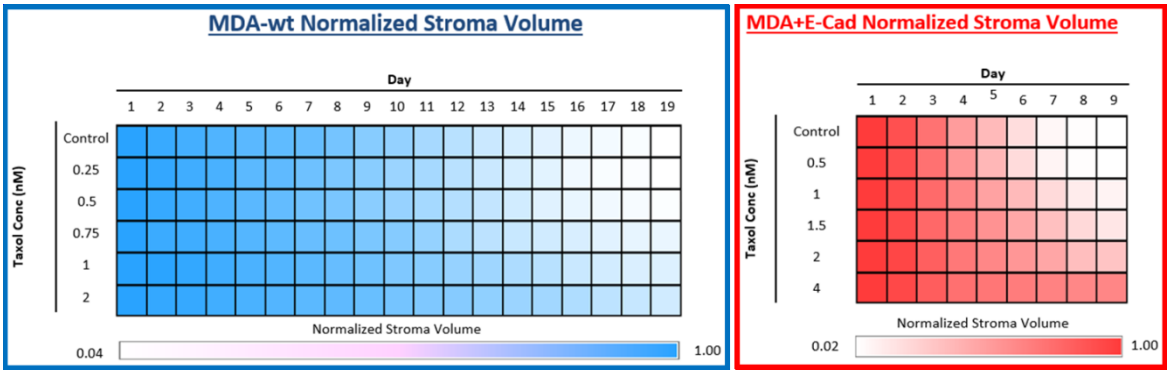

Figure 17: PTX minimizes stroma volume shrinkage in 3DLTS.

3.4 E-Cadherin expression induces higher half maximal inhibitory concentration (IC_{50}) of PTX on MDA-MB-231 tumors

Understanding paclitaxel has an influence on tumor growth and stroma volume shrinkage, we asked whether MDA-wt and MDA+E-Cad would respond differently to the drug. Essentially, we wanted to find out how effective paclitaxel is on MDA-wt vs. MDA+E-Cad. Half maximal inhibitory concentration (IC_{50}) is the concentration of the drug of interest that is needed to inhibit a given biological process by half. Thus, we wanted to use tumor volume, stroma volume, and cell number to elucidate the IC_{50} of paclitaxel across MDA-wt and MDA+E-Cad tumors. Specifically, we asked what is the concentration of paclitaxel that will minimize the tumor volume by half, minimize the stroma volume shrinkage by half, and minimize the cell proliferation (in terms of cell number) by half (Fig. 18). What we found across all three methods is expression of E-Cadherin induces a nearly 3× higher IC_{50} compared to MDA-MB-231 wt tumor spheroids.

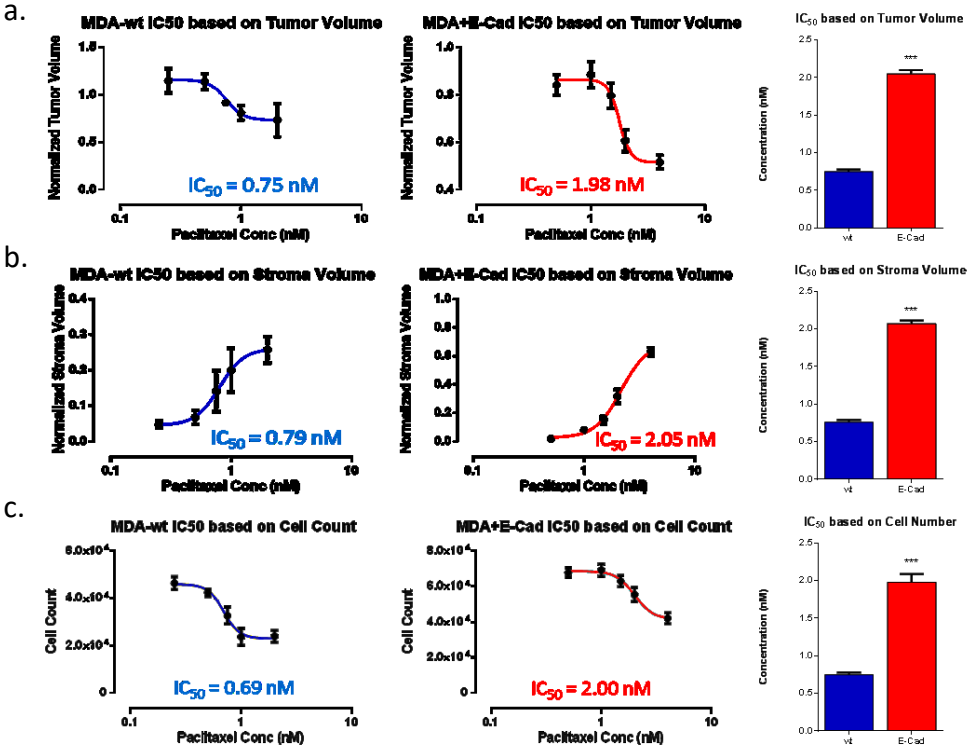

Figure 18: E-Cadherin expression induces higher IC_{50} of PTX on MDA-MB-231 tumors. Whether it is calculating IC_{50} through a. tumor volume, b. stroma volume, or c. cell count, expression of E-Cadherin induces a nearly 3× higher IC_{50} compared to MDA-MB-231 wt tumor spheroids.

On the other hand, when we compared the IC_{50} based on cell count between MDA-wt and MDA+E-Cad on 2D culture, we did not see a significant, if any at all, difference across the two groups (Fig. 19).

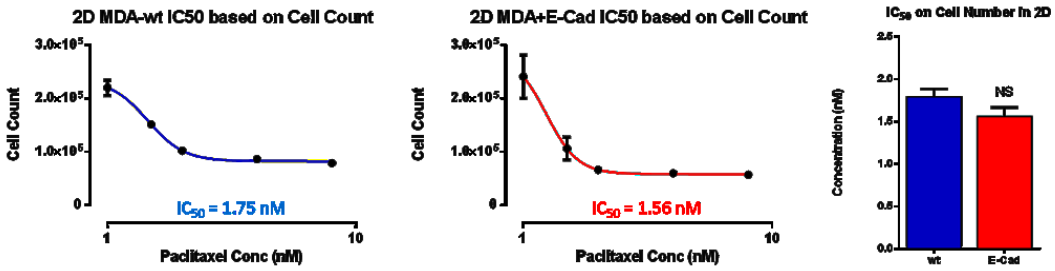

Figure 19: In 2D Culture, E-Cadherin expression does not induce higher IC_{50} of PTX compared to MDA-MB-231 tumors. Expression of E-Cadherin did not induce a significantly different IC_{50} compared to MDA-MB-231 wt cells in 2D culture.

Thus, our 3DLTS was more sensitive in elucidating the different paclitaxel response, and as an *in vitro* tumor model confirms with the clinical observation that overexpression of E-Cadherin has worse prognosis in breast cancer patients, as higher paclitaxel concentration would be needed to induce the same effect on cells without E-Cadherin expression.

3.5 E-Cadherin expression modulates the invasion of MDA-MB-231 tumors

As the tumors grow and invade into the stroma area, the dissemination of cells of MDA-wt and MDA+E-Cad tumors are quite different. The invaded MDA-wt cells were randomly distributed within collagen matrix and were distinguished from the tumor sphere. In contrast, the invaded MDA+E-Cad cells concentrated along tumor sphere and

became part of the tumor sphere, which led to a rapid increase of the volume of MDA+E-cad sphere (Fig. 20a). The images indicated that the presence of E-Cadherin switch MDA-MB-231 cells from individual collective toward frontal invasion and the frontal invasion is more efficient to increase the tumor size comparing to individual collective invasion.

We further characterized the invasion mode by looking at the maximal invasion distance. This distance was determined by the average distance traveled by 20 individual cells furthest away from the tumor mass, as shown in the line drawn (Fig. 20a). We observed due to the individual collective invasion of MDA-wt, the maximal invasion distance of MDA-wt is nearly 3× greater than that of MDA+E-Cad which undergo frontal invasion (Fig. 20b). Though MDA-wt cells may travel further, but the collective forces undergoing frontal migration carried by MDA+E-Cad indicate E-Cadherin led MDA-MB-231 tumors to stick together and rapidly grow into the stromal area.

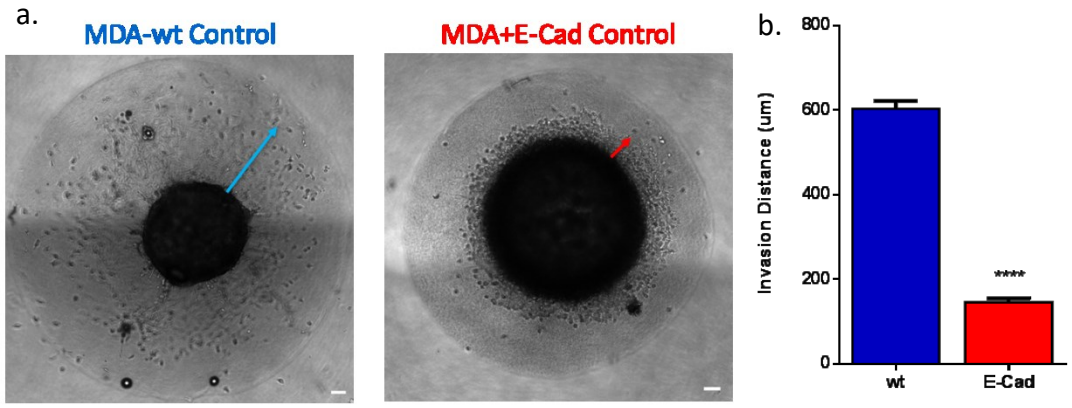

Figure 20: E-Cadherin expression modulates the invasion of MDA-MB-231 tumors. a. Individual collective migration is observed in MDA-wt, whereas frontal invasion is seen in MDA+E-Cad tumors. b. There is a significant difference between the maximal invasion distances of MDA-wt vs. MDA+E-Cad tumors.

3.6 PTX inhibits tumor cell proliferation and invasion in 3DLTS

As we saw the differences of invasion across MDA-wt and MDA+E-Cad, we also wanted to observe how paclitaxel would affect tumor cell proliferation and invasion. Similarly, from imaging, we categorized the maximal invasion distance under the influence of paclitaxel (Fig. 21).

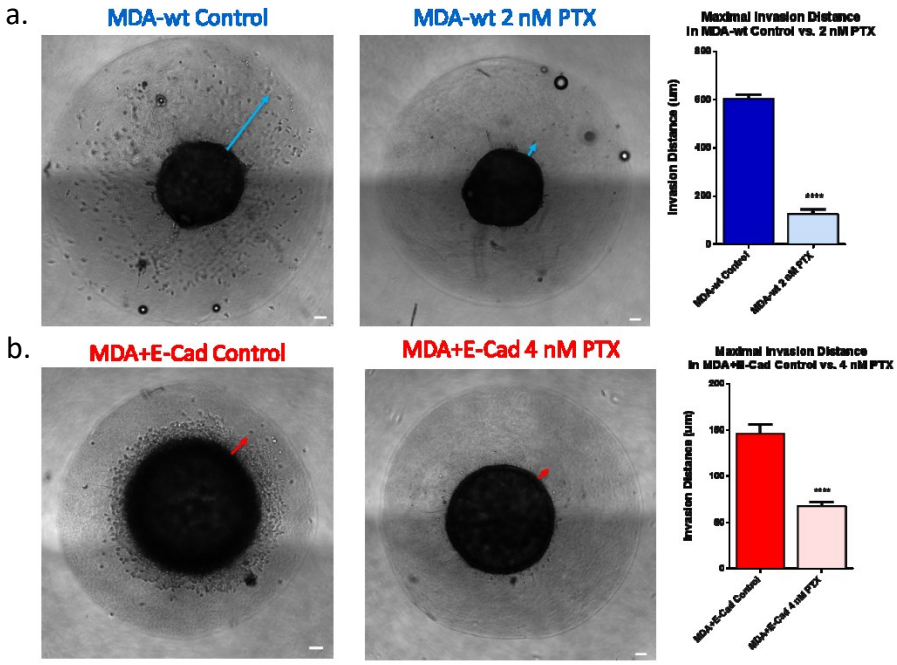

Figure 21: PTX inhibits tumor cell proliferation and invasion in 3DLTS. Whether it is under a. MDA-wt or b. MDA+E-Cad, paclitaxel is able to inhibit invasion, as shown by the decrease in maximal invasion distance.

Under the influence of paclitaxel, tumor invasion is inhibited in MDA-wt and MDA+E-Cad 3DLTS. The maximal invasion distance decreased significantly across both tumor groups. From our 3DLTS, we demonstrated that paclitaxel can inhibit tumor invasion, tumor growth, stroma contraction regardless of E-Cadherin expression in MDA-MB-231 cells.

Conclusion

The study described highlighted using a novel 3D double-layered tumor spheroid system to assess the effects of paclitaxel on carcinoma cells. Our 3DLTS assembled matrigel and collagen gel mimicked the structure and juxtaposed organization of the basement membrane and stromal extracellular matrix, and allowed us to continuously monitor cell proliferation, invasion, collective migration, and tumor growth simultaneously. Our results indicated that 3DLTS recapitulated the rapid growth of E-Cadherin tumor, and that E-Cadherin expression accelerated MDA-MB-231 tumor to compact the surrounding stromal tissue. These results aligned with recent clinical studies which found expression of E-Cadherin functionally supports rapid tumor growth and is associated with poor prognosis.

In addition, we utilized 3DLTS as a drug screening mechanism to closely study the effects of paclitaxel on carcinoma cells. The study concluded paclitaxel was effective in minimizing tumor growth and stroma volume shrinkage in 3DLTS, and E-Cadherin expression induced higher half maximal inhibitory concentration of paclitaxel on MDA-MB-231 tumors. Paclitaxel was also able to inhibit tumor cell proliferation and invasion in 3DLTS.

Our work proved 3DLTS as a novel *in vitro* tumor model that can replicate the tumor microenvironment, and produce results of clinical relevancy. The system has also been proved as an effective drug screening mechanism to lead towards personalized healthcare.

Future Work

Further research will be done to verify the differences of half maximal inhibitory concentration of paclitaxel under E-Cadherin expression in *in vivo* animal models. We elucidated the differences in 2D vs. 3DLTS, and we hope to see similar differences in animal studies. In addition, RNA extraction would be performed to determine gene expression in MDA-wt and MDA+E-Cad at different time points in the tumor progression to further understand which genes are expressed. This work will lead to performing RNA-Seq to study changes in gene expression under different signaling pathways, such as MAPK, TGF_{β}, and Wnt pathways, that have downstream effects in promoting uncontrolled tumor growth.

References

1. American Cancer Society. Cancer Facts & Figures 2016. *Cancer Facts Fig. 2016* (2016): 1-9. doi:10.1097/01.NNR.0000289503.22414.79
2. Godet, I. & Gilkes, D. M. BRCA1 and BRCA2 mutations and treatment strategies for breast cancer. *Integr. Cancer Sci. Ther.* (2017): 5-7.
3. Gilkes, D. M. & Semenza, G. L. Role of hypoxia-inducible factors in breast cancer metastasis. *Future Oncol.* (2013): 1623-37.
4. Slaughter, Danely, et al. "'Field cancerization' in oral stratified squamous epithelium. Clinical implications of multicentric origin." *Cancer* 6.5 (1953): 963-68.
5. Ambrose, J, et al. "Mediated coalescence: a possible mechanism for tumor cellular heterogeneity." *Am J Cancer Res.* 5.11 (2015): 3485-504
6. Chu, Khoi, et al. "The Paradox of E-Cadherin: Role in Response to Hypoxia in the Tumor Microenvironment and Regulation of Energy Metabolism." *Oncotarget* 4.3 (2013): 446-62.
7. Rodriguez, Fausto J., et al. "E-cadherin's Dark Side: Possible Role in Tumor Progression." *Biochimica Et Biophysica Acta (BBA) - Reviews on Cancer* 1826.1 (2012): 23-31
8. Pećina-Slaus, N., et al. "Tumor suppressor gene E-cadherin and its role in normal and malignant cells." *Cancer Cell Int.* 3.17 (2003): 1-7.
9. Perry, Jo K., et al. "Regulation of Invasive Growth: Similar Epigenetic Mechanisms Underpin Tumour Progression and Implantation in Human Pregnancy." *Clinical Science* 118.7 (2010): 451-57
10. Jeanes, A., et al. "Cadherins and Cancer: How Does Cadherin Dysfunction Promote Tumor Progression?" *Oncogene* 27.55 (2008): 6690-929.
11. Byers, SW., et al. "Role of E-cadherin in the response of tumor cell aggregates to lymphatic, venous and arterial flow: measurement of cell-cell adhesion strength." *J Cell Sci*. (1995): 2053-64.
12. Wirtz, Denis, et al. "The Physics of Cancer: The Role of Physical Interactions and Mechanical Forces in Metastasis." *Nature Reviews Cancer* 11.7 (2011): 512-22
13. Weaver, B. A. "How Taxol/paclitaxel Kills Cancer Cells." *Molecular Biology of the Cell* 25.18 (2014): 2677-681.
14. Azouz, S.M., et al. "Prevention of local tumor growth with paclitaxel-loaded microspheres." *J Thorac Cardiovasc Surg.* 135.5 (2008): 1014-21.
15. Katt, Moriah, et al. "In Vitro Tumor Models: Advantages, Disadvantages, variables, and Selecting the Right Platform." *Frontiers in Bioengineering and Biotechnology* 4.12 (2016): 1-7.
16. Ringner, Markus, et al. "GOBO: Gene Expression-Based Outcome for Breast Cancer Online." *PLoS ONE* 6.3 (2011).
17. Gyorffy, Balazs, et al. "An Online Survival Analysis Tool to Rapidly Assess the Effect of 22,277 Genes on Breast Cancer Prognosis Using Microarray Data of 1,809 Patients." *Breast Cancer Research and Treatment* 123.3 (2009): 725-31.

Curriculum Vitae

Eric Tu Ong

110 W. 39th St. Apt. #514 | Baltimore, Maryland 21210

508-863-0116 | ong.eric.tu@gmail.com

Born in Taipei, Taiwan on December 1st, 1993

Son of Hiap Liew Ong and I-An Jennifer Tu

EDUCATION

Johns Hopkins University Baltimore, MD

B.S. in Chemical and Biomolecular Engineering May 2016

Concentration: Molecular & Cellular Bioengineering

M.S.E. in Chemical and Biomolecular Engineering June 2017

SKILLS

- Extensive working experience with Adobe Photoshop, GraphPad Prism, MATLAB, ImageJ, NIS Elements.
- Six-plus years of research lab experience and knowledge of nanoparticle electrochemistry, cell culture, cell counting and sorting, imaging instruments, immunofluorescence microscopy, immunohistochemistry, ELISA, RNA extraction, PCR, Western blot, gel electrophoresis, UV-Vis, DSC, MFI, PTI, CD, DLS, ITC, Tryptophan Fluorescence, RP-HPLC, SEC, ion exchange, affinity, thin-layer chromatography, and others.

RESEARCH & PROFESSIONAL EXPERIENCE

Regeneron Pharmaceuticals Tarrytown, NY

Research Associate II, Protein Biochemistry July 2017 ~ Present

- Conducts biochemical and biophysical characterization experiments on therapeutic protein candidates for late-stage development and regulatory submissions.
- Provides input on experimental design and suggest modifications in protocols or experimental methods to meet the needs of a particular program or molecule.

Institute for NanoBioTechnology, Johns Hopkins University Baltimore, MD

Research Assistant August 2015 ~ June 2017

- Conducted research under Vice Provost for Research Dr. D. Wirtz on utilizing a 3D double-layer tumor spheroid culture system for drug screening. The enhanced method would be high-throughput, cost-effective, and provide an early identification of a drug's effectiveness against the disease.

- Experimented in-vitro 3D cell culture methods of wildtype and E-Cadherin-rich breast epithelial cancerous tumors.

Johns Hopkins Technology Ventures Baltimore, MD

Agreement Monitoring Intern Analyst September 2016 ~ April 2017

- Actively reviewed and analyzed exclusive and non-exclusive licenses, agreements, and Product Pipeline Report.
- Interacted closely with licensing associates on licensed cases and with Finance Department with financial data of agreements and other projects as assigned.

MedImmune, AstraZeneca Gaithersburg, MD

Formulation Sciences Intern June 2016 ~ August 2016

- Conducted research on the effect of buffers in formulation development through formulation screening, optimization, excipient testing, and stability studies of monoclonal antibodies immersed in various formulations.
- Presented at intern, group, and department meetings, as well as poster sessions during the 12-week internship.

Department of ChemBE, Johns Hopkins University Baltimore, MD

Research Assistant January 2013 ~ April 2016

- Conducted research under Dr. J. Frechette on the electrochemical control of gold-nanoparticles at oil-water interface, and presented poster sessions and gives lab presentations to research groups.
- Awarded Provost's Undergraduate Research Awards.

Syncore Biotechnology, Sinphar Group Taipei, Taiwan

Business Development Intern/Consultant July 2015 ~ December 2015

- Researched biotechnology companies and pharmaceuticals new drug pipeline process, and identified potential partners for the company's five line of products.
- Analyzed journals for scientific background and relevancy to Syncore's products for sales representatives to use.

TTY Biopharm Chungli, Taiwan

Operation & Production Intern May 2015 ~ July 2015

- Shadowed managers from different departments (Operation, Production, Validation, QA/QC, Factory Affairs, and Engineering) and assisted factory operations in oncology vaccination and capsule production.
- Presented to department managers and operation director on overall factory analysis and future scope.

LEADERSHIP EXPERIENCE

Study Consultant, Office of Academic Advising Fall 2016 ~ Spring 2017

- Worked one-on-one with undergraduate students on global academic skills such as time management, note-taking skills, organization, test

preparation, and other skills to help students adjust to the increased demands of college.

Commissioner, Student Government Association Fall 2013 ~ Spring 2016

- Reviewed and approved monthly ($60 K) and annual ($350 K) grants submitted by 450+ student groups.
- Served as an advisor to 80 student groups to help allocate and review their funding.

USG of ECOSOC, JHUMUNC Fall 2012 ~ Spring 2016

- Led 18 committees with 2,000+ international high school students and 170+ staff members for over 4 day conference in Hilton Baltimore, and ran weekly meetings with staff to cover parliamentary procedures.

President, Taiwanese American Student Association Fall 2012 ~ Spring 2016

- Led weekly board meetings and organized events for 400+ members and governed $7,000 annual budget.

HONORS

Provost's Undergraduate Research Awards 2014

Highly selective $2,500 fellowship to award innovative and breakthrough projects designed by an undergraduate.

ChemBE Undergraduate Research Accomplishments 2014, 2015

Best Product Concept at ChemBE Product Design Poster Session 2016

Dean's List for Academic Excellence

Dean's Master's Fellowship